Proc. Natl. Acad. Sci. USA
Vol. 85, pp. 4548–4552, June 1988
Neurobiology

Ion transport by the Na–Ca exchange in isolated rod outer segments

(electrogenic carrier/membrane potential/retina)

L. LAGNADO*, L. CERVETTO†, AND P. A. MCNAUGHTON*‡

*Physiological Laboratory, Downing Street, Cambridge CB2 3EG, United Kingdom; and †Istituto di Neurofisiologia, Consiglio Nazionale delle Ricerche, via San Zeno 51, 56100 Pisa, Italy

Communicated by A. L. Hodgkin, March 1, 1988

ABSTRACT **The inward membrane current generated by the coupled exchange of external sodium for internal calcium has been investigated in isolated rod outer segments. The exchange rate is sensitive to voltage, with a reduction by a factor of *e* occurring for a 70-mV depolarization in normal Ringer's solution. The voltage sensitivity is not a constant property of the exchange, as it is reduced by an increase in external Na^+ or by the removal of external Ca^{2+}, Mg^{2+}, or K^+. Changes in membrane potential do not appear to affect the affinity of the exchange mechanism for internal Ca^{2+}, but hyperpolarization increases the affinity for external Na^+. When the external Na^+ concentration is raised sufficiently to saturate the exchange mechanism, the voltage sensitivity is no longer apparent. We propose that the voltage dependence of the exchange is due to the external Na^+-binding site being sensitive to membrane potential, perhaps because it is located within the membrane electric field.**

A Na–Ca exchange mechanism plays a major role in regulating free internal Ca^{2+} in many types of animal cells, including nerve (1) and muscle (2). The electrical activity of these cells controls such Ca^{2+}-dependent processes as secretion and contraction, partly by regulating Ca^{2+} influx through ion channels, but also by altering Ca^{2+} efflux through the Na–Ca exchange (3–5). Information on the interaction between membrane potential and the exchange is therefore essential to understanding the control of free Ca^{2+} in excitable cells. The effects of voltage on the properties of the Na–Ca exchange may also shed light on the mechanism of ion transport by this carrier.

A major problem in such investigations has been the separation of ion fluxes or membrane currents through the exchange from those through other voltage-dependent pores or carriers (3, 5). We have developed a preparation, the isolated outer segment of rod photoreceptors, that is particularly suited to the study of Na–Ca exchange since only two mechanisms contribute in any appreciable degree to membrane current: the light-sensitive channel, which can be used to load the rod with Ca^{2+} and then closed with a bright light, and the Na–Ca exchange. We have used this preparation to investigate the effects of membrane potential, external Na^+, and internal Ca^{2+} on the inward current generated by the Na–Ca exchange.

METHODS AND MATERIALS

Preparation. Rod outer segments, separated from their inner segments, were mechanically isolated from the retina of the tiger salamander and were held in the mouth of a suction pipette (see Fig. 1*A Inset*), leaving the plasma membrane exposed to a flowing solution that could be changed in 50–100 msec by using an automated multipipe system (6, 7).

Electrical Recording. A whole-cell pipette was used to record membrane current while controlling the membrane potential V_m (8). The whole-cell pipette also maintained the transmembrane Na^+ gradient in the absence of Na–K pumps in the outer segment membrane (9) and supplied the ATP and GTP required by the machinery of phototransduction (10, 11).

Whole-cell pipettes with a resistance of 4–10 MΩ were prepared on a BB-CH puller (Mechanex, Geneva), and recordings were made with a Dagan patch-clamp amplifier (model 8900, Dagan Instruments, Minneapolis, MN) with a 0.1-GΩ feedback resistor in the headstage.

Solutions. Composition of normal Ringer's solution was 110 mM NaCl, 2.5 mM KCl, 1.6 mM $MgCl_2$, 1 mM $CaCl_2$, 10 mM Hepes, neutralized to pH 7.6 with tetramethylammonium hydroxide. For Ca-free and divalent cation-free solutions, the $CaCl_2$ and $MgCl_2$ were omitted and 1 mM EGTA or 1 mM EDTA was added as appropriate; for reduced Na solutions NaCl was replaced with LiCl, which does not activate the exchange (12). The isotonic $CaCl_2$ solution used for introducing a Ca load contained 77.5 mM $CaCl_2$, 0.5 mM 3-isobutyl-1-methylxanthine, 10 mM Hepes (pH 7.6). The suction pipette was filled with solution containing 110 mM Li and nominally zero Ca to prevent activation of the Na–Ca exchange, in either the forward or the backward mode, in the small area of membrane within the suction pipette mouth. Whole-cell pipettes were filled with a Na-free solution containing 110 mM potassium aspartate, 3 mM $MgCl_2$, 1 mM K_2ATP, 1 mM Li_2GTP, 0.06 mM cGMP, 0.02 mM bis(2-aminophenoxy)ethane-*N,N,N′,N′*-tetraacetate (BAPTA), 10 mM Pipes, neutralized to pH 7.2 with KOH. The junction potential at the whole-cell pipette mouth between this solution and Ringer's was found to be −14 mV, and all measured membrane potentials have been corrected appropriately.

RESULTS

The protocol for loading the rod outer segment with a known amount of Ca^{2+} and for measuring the Na–Ca exchange current is shown in Fig. 1*A*. The rod was first exposed to a loading solution, in which Ca^{2+} is the only permeant ion, to cause a Ca^{2+} influx through the light-sensitive channels. The influx was terminated by a bright step of light and the Ca^{2+} load within the rod was measured directly as the integral of the inward current during the loading period. The current recorded on return to a Na^+-containing solution has been shown to be due to the operation of an electrogenic Na–Ca exchange (7, 11–17). This current remained saturated for a length of time that depended on the Ca^{2+} load and then declined to zero as the load was removed. If the bright light was maintained after removal of Ca^{2+} the input resistance of

The publication costs of this article were defrayed in part by page charge payment. This article must therefore be hereby marked "*advertisement*" in accordance with 18 U.S.C. §1734 solely to indicate this fact.

‡To whom reprint requests should be addressed.

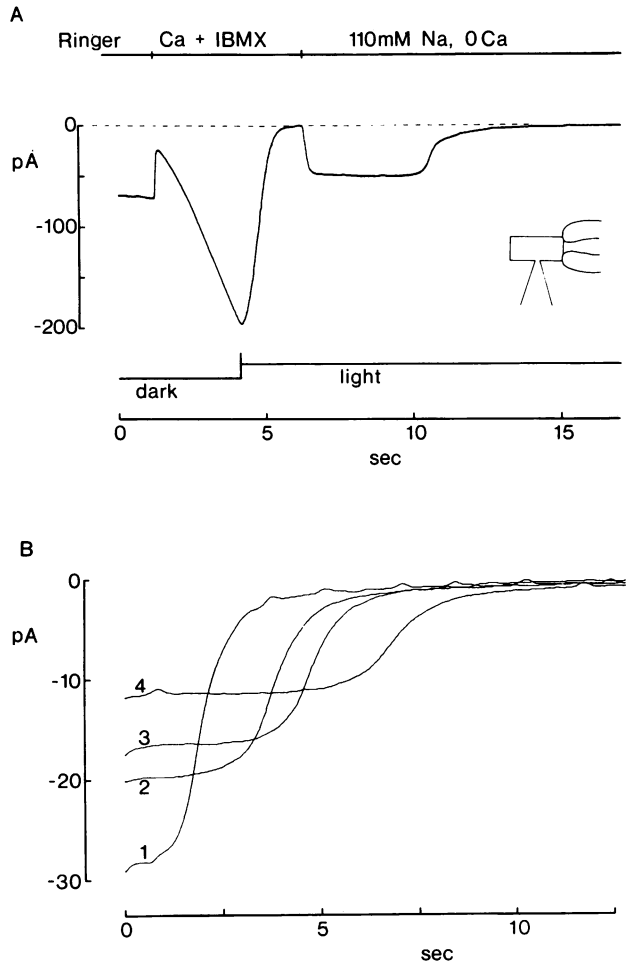

FIG. 1. (*A*) Isolation of the Na–Ca exchange current in a rod outer segment. (*Inset*) Experimental arrangement; the suction pipette, to the right, is used to hold the rod in the stream of flowing solution, while the whole-cell pipette, shown below the rod, maintains electrical continuity with the rod cytoplasm. V_m was clamped to −14 mV throughout. Solution changes are shown above current record; light monitor is shown below. The rod was exposed first to a "loading solution" containing isotonic $CaCl_2$ and the phosphodiesterase inhibitor 3-isobutyl-1-methylxanthine (IBMX). Elevation of external Ca^{2+} caused an initial rapid suppression of current due to an external action on light-sensitive channels. The subsequent increase of inward Ca^{2+} current occurs because the inhibition of cGMP hydrolysis in the presence of IBMX causes the cGMP-gated light-sensitive channels to open (7). Ca^{2+} influx was terminated by a bright flash (1900 photons·μm^{-2}; 500 nm) followed by a continuous light step to hold the light-sensitive current suppressed (613 photons·μm^{-2}·sec^{-1}; 500 nm). The Na–Ca exchange current was then activated by transfer to a solution containing 110 mM Na and 0 mM Ca. Charge transferred during loading, 417.5 pC; charge transferred during exchange, 220.0 pC, so the measured exchange stoichiometry was 3.05 Na^+/1 Ca^{2+}. (*B*) The Na–Ca exchange current under various conditions, recorded as in *A* but in a different rod. At the end of the loading period, 1 sec before exchange was initiated by the application of external Na, the membrane potential V_m was stepped from a holding level of −14 mV. $[Na]_o$ and V_m were 110 and −64 mV (curve 1); 110 and −14 mV (curve 2); 75 and −64 mV (curve 3); 75 and −14 mV (curve 4). Measured exchange stoichiometries were 2.99 (curve 1), 3.00 (curve 2), 3.05 (curve 3) and 2.96 (curve 4). Curves were smoothed by convolution with a Gaussian filter of standard deviation 100 msec.

the preparation became as high as 40 GΩ, confirming that all channels in the outer segment membrane are blocked by light (11, 18, 19). An uncontaminated Na–Ca exchange current can therefore be recorded without resorting to subtraction procedures or to pharmacological blockers of other membrane currents.

Examples of the effects of changes in membrane potential (V_m) or the external Na^+ concentration ($[Na]_o$) on the exchange current are shown in Fig. 1*B*. A 50-mV hyperpolarization increased the saturated exchange current and accelerated the removal of a Ca^{2+} load. Reducing $[Na]_o$ from 110 to 75 mM reduced the saturated exchange current and slowed the removal of a Ca^{2+} load. These changes in the magnitude of the current were not due to changes in the stoichiometry of the exchange, which can be measured from the ratio between the total Ca^{2+} influx during the loading period and the total charge transported by the exchange during the extrusion of the Ca^{2+} load (7, 13, 14). In 45 measurements on five rods with $[Na]_o$ ranging from 35 to 220 mM, V_m from −64 to +16 mV, and $[Ca]_o$ = 0 or 1 mM, the value of the exchange ratio (mean ± SEM) was 3.013 ± 0.01 Na^+ ions entering per Ca^{2+} ion extruded from the cell (see also refs. 7, 13, 14, and 20). We conclude that the exchange has a fixed Na^+/Ca^{2+} stoichiometry of 3:1.

Voltage Dependence in Physiological Conditions. The sensitivity of the Na–Ca exchange to membrane potential was first investigated in normal Ringer's solution (Fig. 2). Hyperpolarization increased the exchange current observed with saturating concentrations of internal Ca^{2+} ($[Ca]_i$), and over the range V_m = −74 to +36 mV the rate of exchange showed an exponential dependence on membrane potential with an *e*-fold change occurring in 70 mV. The exchange current at a membrane potential V_2, $j(V_2)$, is therefore related to that at V_1 by $j(V_2) = j(V_1)\exp[(V_1 - V_2)/70]$. Because the effect of V_m on the exchange rate is independent of $[Ca]_i$ (see below), this relationship defines the voltage dependence of Na_o/Ca_i exchange for all $[Ca]_i$, including the physiological range. An important prediction of these results is that the hyperpolarization following an intact rod's response to light will accelerate Ca^{2+} efflux from the outer segment and therefore speed the decrease in $[Ca]_i$ that is thought to mediate adaptation to light (14, 21–25).

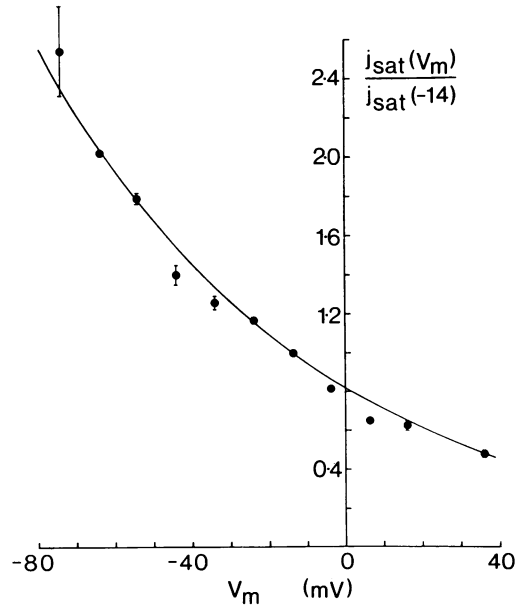

FIG. 2. Voltage dependence of the Na–Ca exchange in normal Ringer's solution containing 1 mM Ca. The exchange current, $j_{sat}(V_m)$, which is recorded at a membrane potential V_m after a Ca load sufficient to saturate the internal Ca-binding site, is expressed relative to the amplitude observed at −14 mV in each experiment. Points are mean values, with error bars showing ±SEM. Points at −4 mV and −16 mV are single observations. Collected results from 66 measurements on six cells. Continuous line is $j_{sat}(V_m)/j_{sat}$ (−14 mV) = $\exp[-(V_m + 14)/70]$ (see text).

Activation by Internal Calcium. It is clear that changes in the affinity of the internal Ca^{2+}-binding site cannot account for the dependence of exchange current on membrane potential shown in Fig. 2, since this relationship was obtained with $[Ca]_i$ at saturating levels. It is nonetheless possible that membrane potential might affect the binding of Ca^{2+} and therefore cause the voltage sensitivity of the exchange to depend on the $[Ca]_i$ at which it is measured. This possibility was investigated by the method shown in Fig. 3. By directly measuring free Ca^{2+} in intact rods with aequorin we have shown that the exchange current j is activated in a first-order manner with a Michaelis constant, K_m, of 2.3 μM (15). We have assumed that this relationship also holds at -14 mV in 110 mM Na and 0 mM Ca (Fig. 3, curve 2):

$$\frac{j}{j_{sat}} = \frac{[Ca]_i}{[Ca]_i + K_m}. \quad [1]$$

The total exchangeable [Ca], $[Ca]_T$, remaining within the rod outer segment at time t during the extrusion of a Ca^{2+} load can also be calculated by integrating the exchange current:

$$[Ca]_T = (1/FV)\int_t^\infty j\,dt', \quad [2]$$

and therefore the relationship between the free and total exchangeable Ca in the rod can be obtained:

$$[Ca]_i = B([Ca]_T), \quad [3]$$

where B defines the buffering power of the cytoplasm as a function of $[Ca]_i$, and V is the outer segment volume. The intracellular buffers act rapidly and reversibly (14), so B is effectively time independent. The dependence of the exchange current on $[Ca]_i$ at other membrane potentials and in other external ionic conditions can then be computed by using the relationship B to convert $[Ca]_T$ to $[Ca]_i$. The results of this calculation are shown in Fig. 3. The continuous lines close to each set of points show Michaelis relationships with K_m = 2.3 μM. The good fit demonstrates that the activation of the exchange by internal Ca^{2+} ions is independent of the effects of membrane potential or changes in external Na^+. Similar results were obtained in eight cells over the ranges V_m = -64 to $+16$ mV and $[Na]_o$ = 220 to 55 mM. These observations show that the internal Ca^{2+}-binding site is unaffected by the membrane electric field and that Ca^{2+} binding internally proceeds independently of Na^+ binding externally (12, 16).

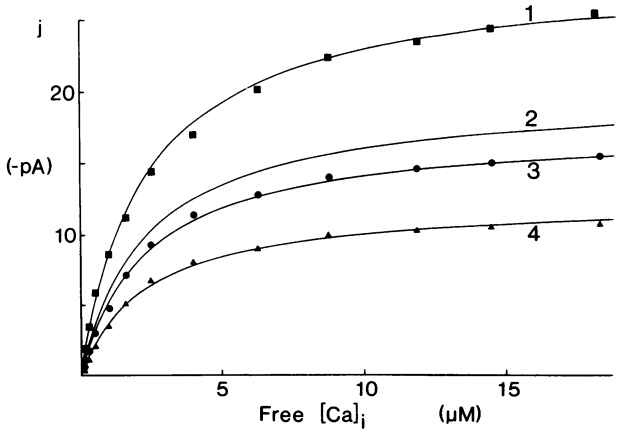

FIG. 3. Activation of the Na–Ca exchange current by internal Ca^{2+}. The exchange current j is plotted as a function of free $[Ca]_i$, obtained as described in the text (Eqs. 1–3). Data are from Fig. 1*B*, with the same numbering system.

Voltage Dependence of External Sodium Binding. A second site at which membrane potential might act on the exchange is the binding of Na^+ ions at the external membrane surface. To investigate this possibility, the activation of the exchange current by external Na^+ was first characterized at a constant membrane potential of -14 mV (Fig. 4*A*, curve 1). All competing cations (Ca^{2+}, Mg^{2+}, K^+) were removed from the external solution to maximize the Na^+ affinity of the exchange mechanism. The activation curve was best described by a Hill equation of the form

$$\frac{j'}{j'_{max}} = \frac{[Na]_o^h}{[Na]_o^h + K_{1/2}^h}, \quad [4]$$

where j' is the exchange current at a saturating level of $[Ca]_i$, normalized to its value in 110 mM Na and 0 mM Ca at -14 mV; $K_{1/2}$ is the $[Na]_o$ giving half-maximal activation of the exchange current; and h is the Hill coefficient. The constant j'_{max} is the magnitude of j' when the external Na^+-binding site is fully saturated. The best straight-line fit to a Hill plot was obtained by taking j'_{max} to be 2.66, as shown in Fig. 4*B*. The values of h and $K_{1/2}$ measured from this plot were 2.26 and 93

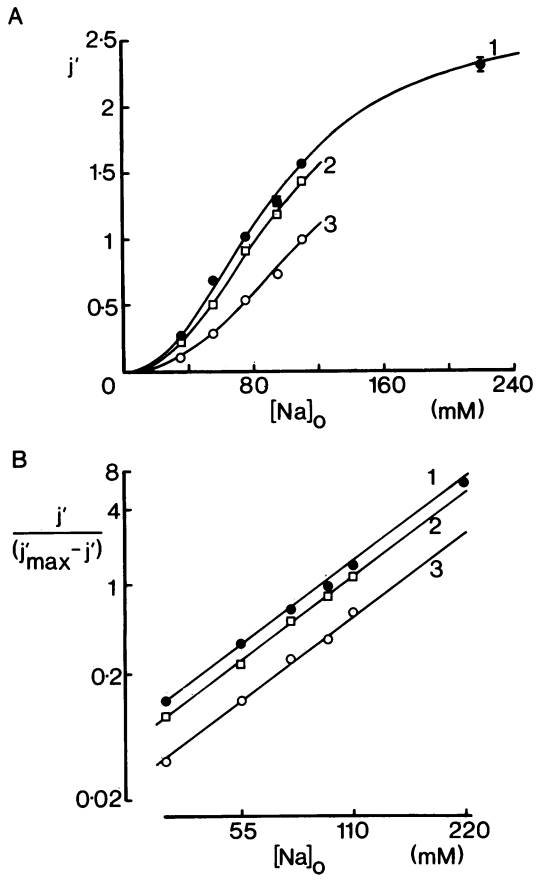

FIG. 4. Dependence of the Na–Ca exchange current on $[Na]_o$, and the effects of hyperpolarization. (*A*) ●, V_m = -14 mV; 0 mM Ca, 0 mM Mg, 0 mM K. Curve 1 fitted to points according to Eq. 4 in text with j'_{max} = 2.66, h = 2.26, and $K_{1/2}$ = 93 mM. Hypertonicity of the 220 mM Na solution had no effect on the exchange, because identical activation was observed in solutions containing 110 mM Na and 110 mM Na plus 110 mM Li. □, V_m = -64 mV; 0 mM Ca, 1.6 mM Mg, 2.5 mM K. Curve 2 fitted to points with j'_{max} = 2.66, h = 2.26, $K_{1/2}$ = 103 mM. ○, V_m = -14 mV; 0 mM Ca, 1.6 mM Mg, 2.5 mM K. Curve 3 fitted to points with j'_{max} = 2.66, h = 2.26, $K_{1/2}$ = 139 mM. Error bars show ± SEM where large enough to illustrate; in other cases the SEM is less than the point size. Collected results are from 102 measurements on eight cells. (*B*) Hill plot of data shown in *A*. Same symbols and numbering system. Straight-line fits were drawn by eye, using j'_{max} = 2.66.

mM, respectively. An h value of <3 might be explained if the Na^+-binding sites were not equivalent (see also refs. 12, 26, and 27).

The effects of membrane potential on the activation of the exchange by external Na^+ were investigated in the presence of Mg^{2+} and K^+, when stable recordings were more easily obtained. The activation by Na^+ at -14 mV (Fig. 4*A*, curve 3) could be described by using the same value of j'_{max}, when a good straight-line fit to a Hill plot was obtained (Fig. 4*B*). The Hill coefficient measured in this way was the same as in the absence of Mg^{2+} and K^+, but the $K_{1/2}$ increased to 139 mM, consistent with a simple competition between these ions and external Na^+ (12). The effect of hyperpolarization to -64 mV, shown as curve 2 in Fig. 4*A*, was to increase the affinity for external Na^+, the $K_{1/2}$ being reduced to 103 mM. Hyperpolarization did not appear to change either the maximum rate of the exchange mechanism or the Hill coefficient of activation. The effect of hyperpolarization, therefore, depends on the external Na^+ concentration, becoming less as $[Na]_o$ is increased.

This surprising effect is explored more fully in Fig. 5*A*. The continuous curve is the voltage dependence of the exchange in Ringer's solution, taken from Fig. 2, and the points show the voltage dependence in a variety of other external ionic conditions. The voltage sensitivity is clearly not a constant property of the exchange, being reduced by an increase in $[Na]_o$ or by the removal of competing cations. This effect can be quantified by using the parameter j' (Eq. 4), which is directly proportional to the degree to which the Na^+-binding site is saturated. Fig. 5*B* shows that the voltage sensitivity of the exchange declines linearly as the value of j' increases toward a maximum value of ≈2.35. The voltage indepen-

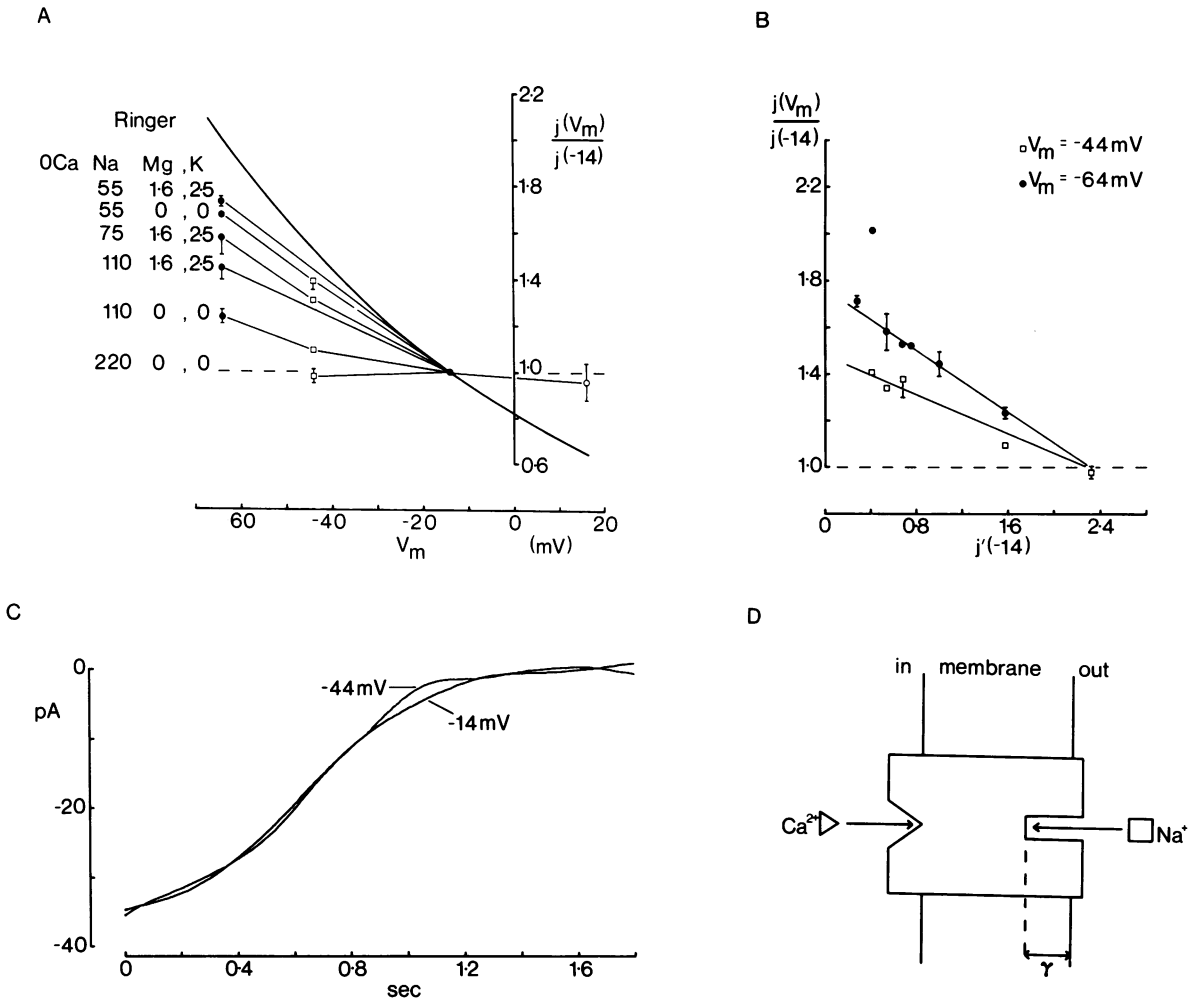

FIG. 5. Voltage dependence of Na–Ca exchange current under various external ionic conditions. (*A*) Exchange current at a potential V_m, $j(V_m)$, is plotted relative to its magnitude at -14 mV. This ratio was independent of the Ca^{2+} load at which it was measured (see Fig. 3 and text), but for convenience it was calculated with saturating levels of $[Ca]_i$. The curve is that fitted to the data in Ringer's solution in Fig. 3. The external ionic concentrations (mM) are shown beside each set of points, which have been connected by straight lines. ●, 50 mV hyperpolarization; □, 30 mV hyperpolarization. Bars show ±SEM. Collected results are from 60 measurements on seven cells, not including those in Ringer's solution. (*B*) Activation of the exchange current on hyperpolarization expressed as a function of its normalized value at -14 mV, $j'(-14)$. The saturated exchange current under a given ionic condition was normalized relative to the saturated current in 110 mM Na and 0 mM Ca at -14 mV. The parameter $j'(-14)$ is directly proportional to the degree to which the Na^+-binding site is saturated (see Eq. 4). Symbols are the same as in *A*. The intercepts with the voltage-independent limit (shown by dashed line) are 2.36 for a 50-mV hyperpolarization, and 2.32 for a 30-mV hyperpolarization. The voltage sensitivity in the presence of 1 mM external Ca^{2+} (upper point) is significantly greater than predicted by the linear relationship obtained in 0 mM Ca, possibly because Ca^{2+} competes with more than two Na^+ ions. The majority of the data are from *A*. (*C*) Voltage-independence of the Na–Ca exchange current in 220 mM Na in the absence of other external cations. Curves were smoothed by convolution with a Gaussian filter of standard deviation 100 msec. (*D*) Schematic diagram of the Na–Ca exchange molecule showing the proposed locations of the Na^+- and Ca^{2+}-binding sites of the unloaded carrier; for the purposes of illustration only, one Na^+-binding site is shown. γ, Fraction of the transmembrane potential sensed by a Na^+ ion on binding at the external membrane surface. The internal Ca^{2+}-binding site is outside the membrane electric field.

dence of the exchange when the Na^+-binding site is near saturation is illustrated by Fig. 5*C*, which shows exchange currents recorded at −14 and −44 mV in 220 mM Na in the absence of other external cations. In normal Ringer's solution the same hyperpolarization increases the exchange rate by a factor of 1.54 and correspondingly speeds the extrusion of a Ca load (see Figs. 1 and 2).

The action of membrane potential on the affinity for external Na^+ does not depend on the rate at which the exchange operates. As shown in Fig. 3, the effect of changing $[Na]_o$ or V_m is unaltered as $[Ca]_i$ decreases and the exchange rate is reduced. This is also shown in Fig. 5*C*, where hyperpolarization has little effect on the exchange current both with high $[Ca]_i$, at the start of the record, and later as $[Ca]_i$ is reduced by the action of the exchange. The simplest explanation of the effects observed in Figs. 4 and 5 is that hyperpolarization increases the affinity of the external Na^+-binding site. This might arise if the site were located within the membrane, sensing a fraction, γ, of the membrane electric field, as shown in Fig. 5*D*.

DISCUSSION

The use of isolated rod outer segments has allowed us to characterize some fundamental properties of the Na–Ca exchange carrier, including the stoichiometry and the interactions of external Na^+, internal Ca^{2+}, and membrane potential with the exchange. The most surprising observation is that the voltage sensitivity of the exchange is dependent on the degree to which the Na^+-binding site is saturated but is independent of its activation by internal Ca^{2+}. The effects of a hyperpolarization could be simply accounted for by an increase in the affinity for external Na^+, and at saturating Na^+ concentrations the rate of exchange was found to be independent of membrane potential. This leads us to conclude that the voltage-dependent binding of external Na^+ ions is the process conferring voltage sensitivity on the Na–Ca exchange.

The demonstration that the translocation of a charged species is voltage independent may seem contradictory but can be explained if the rate at which the exchange mechanism operates is determined by a rate-limiting step that does not involve the movement of charge across the membrane electric field. The exchange cycle probably involves a series of reactions, any one of which may be rate limiting but insensitive to voltage. Unfortunately, unlike other membrane carriers such as the Na^+,K^+-ATPase, very little is known at present about the molecular mechanism of the Na–Ca exchange.

These results may give some insight into the structure of the carrier molecule (Fig. 5*D*). The voltage insensitivity of Ca^{2+} binding at the internal membrane surface suggests that the Ca^{2+}-binding site projects beyond the membrane electric field into the cytoplasm. In contrast, the binding of external Na^+ ions *is* sensitive to voltage, indicating that the Na^+-binding site is within the membrane field.

We thank A. L. Hodgkin, B. J. Nunn, and W. G. Owen for many helpful discussions, and I. M. Glynn, T. D. Lamb, and R. J. Perry for their comments on the manuscript. This work was supported by the Medical Research Council and the Wellcome Trust. L.L. is a George Henry Lewes Student.

1. Blaustein, M. P. & Hodgkin, A. L. (1969) *J. Physiol. (London)* **200,** 497–527.
2. Reuter, H. & Seitz, N. (1968) *J. Physiol. (London)* **195,** 451–470.
3. Pott, L. (1986) *Trends Pharmacol. Sci.* **7,** 296–297.
4. Allen, T. J. A. & Baker, P. F. (1987) *J. Physiol. (London)* **378,** 77–96.
5. Kimura, J., Miyamae, S. & Noma, A. (1987) *J. Physiol. (London)* **384,** 199–222.
6. Hodgkin, A. L., McNaughton, P. A. & Nunn, B. J. (1985) *J. Physiol. (London)* **358,** 447–468.
7. Hodgkin, A. L., McNaughton, P. A. & Nunn, B. J. (1987) *J. Physiol. (London)* **391,** 347–370.
8. Hamill, O. P., Marty, A., Neher, E., Sakmann, B. & Sigworth, F. J. (1981) *Pflügers Arch.* **395,** 6–18.
9. Spencer, M. P., Detwiler, P. B. & Bunt-Milam, A. H. (1986) *Invest. Ophthalmol. Vis. Sci.* **235,** Suppl. 27(3).
10. Sather, W. A. & Detwiler, P. B. (1987) *Proc. Natl. Acad. Sci. USA* **84,** 9290–9294.
11. Lagnado, L. & McNaughton, P. A. (1987) *J. Physiol. (London)* **390,** 11P.
12. Hodgkin, A. L. & Nunn, B. J. (1987) *J. Physiol. (London)* **391,** 371–398.
13. Yau, K.-W. & Nakatani, K. (1984) *Nature (London)* **311,** 661–663.
14. McNaughton, P. A., Cervetto, L. & Nunn, B. J. (1986) *Nature (London)* **322,** 261–263.
15. Cervetto, L., Lagnado, L. & McNaughton, P. A. (1987) *J. Physiol. (London)* **382,** 135P.
16. Lagnado, L. & McNaughton, P. A. (1987) *J. Physiol. (London)* **390,** 162P.
17. Nakatani, K. & Yau, K.-W. (1988) *J. Physiol. (London)* **395,** 695–729.
18. Baylor, D. A. & Lamb, T. D. (1982) *J. Physiol. (London)* **328,** 49–71.
19. Baylor, D. A. & Nunn, B. J. (1986) *J. Physiol. (London)* **371,** 115–145
20. Reeves, J. P. & Hale, C. C. (1984) *J. Biol. Chem.* **259,** 7733–7739.
21. Yau, K.-W. & Nakatani, K. (1985) *Nature (London)* **313,** 579–582.
22. Robinson, P. R., Kawamura, S., Abramson, B. & Bownds, M. D. (1980) *J. Gen. Physiol.* **76,** 631–645.
23. Cervetto, L., Torre, V., Rispoli, G. & Marroni, P. (1985) *Exp. Biol.* **44,** 147–157.
24. Torre, V., Matthews, H. R. & Lamb, T. D. (1986) *Proc. Natl. Acad. Sci. USA* **83,** 7109–7113.
25. McNaughton, P. A. & Cervetto, L. (1986) *Photobiochem. Photobiophys.* **13,** 399–414.
26. Baker, P. F. & McNaughton, P. A. (1976) *J. Physiol. (London)* **259,** 103–144.
27. Reeves, J. P. & Sutko, J. L. (1983) *J. Biol. Chem.* **258,** 3178–3182.